arXiv:2512.17637v1 [cs.AI] 19 Dec 2025

About Time: Model-free Reinforcement Learning with Timed Reward Machines

Anirban Majumdar[1], Ritam Raha[2], Rajarshi Roy[3],
David Parker[3], and Marta Kwiatkowska[3]

[1]Tata Institute of Fundamental Research, India
[2]Max Planck Institute for Software Systems, Germany
[3]Department of Computer Science, University of Oxford, UK

Abstract

Reward specification plays a central role in reinforcement learning (RL), guiding the agent's behavior. To express non-Markovian rewards, formalisms such as reward machines have been introduced to capture dependencies on histories. However, traditional reward machines lack the ability to model precise timing constraints, limiting their use in time-sensitive applications. In this paper, we propose timed reward machines (TRMs), which are an extension of reward machines that incorporate timing constraints into the reward structure. TRMs enable more expressive specifications with tunable reward logic, for example, imposing costs for delays and granting rewards for timely actions. We study model-free RL frameworks (i.e., tabular Q-learning) for learning optimal policies with TRMs under digital and real-time semantics. Our algorithms integrate the TRM into learning via abstractions of timed automata, and employ counterfactual-imagining heuristics that exploit the structure of the TRM to improve the search. Experimentally, we demonstrate that our algorithm learns policies that achieve high rewards while satisfying the timing constraints specified by the TRM on popular RL benchmarks. Moreover, we conduct comparative studies of performance under different TRM semantics, along with ablations that highlight the benefits of counterfactual-imagining.

Keywords: Timed Automata, Reinforcement Learning, Reward Machines

1 Introduction

Reinforcement Learning (RL) [33, 35] has become a foundational paradigm for sequential decision-making, enabling agents to learn optimal behavior through interactions with an environment. A crucial aspect of any RL problem is the reward specification, which defines the agent's learning objective. Traditionally, rewards are assumed to depend only on the current state and action, conforming to the Markov property. However, many real-world tasks require objectives that depend on the history of states, such as completing a sequence of goals or avoiding repeated errors. To address this, non-Markovian reward formalisms have been developed, with reward machines (RMs) emerging as a prominent approach.

Reward machines [26, 27] use finite-state automata to specify structured, history-dependent reward functions. They provide a compact and expressive way to encode high-level objectives and have been successfully integrated into RL frameworks, improving sample efficiency and interpretability. However, a critical limitation of existing reward machines is their inability to express timing

constraints—a vital requirement in domains such as robotics and autonomous driving [30], where requirements often involve time-sensitive elements. For instance, an AV might need to "respond to a pedestrian crossing signal within 3 seconds" or "avoid an unsafe road for at least 10 seconds".

In this paper, we propose Timed Reward Machines (TRMs), an extension of reward machines that integrates timing constraints into the reward specification. TRMs allow reward functions to depend not only on the agent's history of actions and states, but also on the time intervals between events. Moreover, TRMs can assign costs and rewards to states and transitions, incentivizing the agent to perform a task while respecting timing constraints and optimizing the overall reward simultaneously.

To illustrate the setting, we define a simple TRM objective (Figure 1b) on the standard Taxi domain (Figure 1a). The TRM encourages an agent (a taxi) to drive slowly, for example, due to heavy traffic, by providing a higher reward when the agent delays at each step (enforced by a self-loop with a timing constraint of $x > 1$). Additionally, it imposes a deadline for picking up the passenger (enforced by a transition with timing constraint $y \leq 14$). Finally, after pickup, the agent must reach the destination (while driving slowly). Such time-sensitive objectives, involving delays and deadlines, can be naturally captured by TRMs.

We interpret TRMs over Markov decision processes (MDPs) to model stochastic environments (Section 3). To express timing constraints, we augment the MDP action set with explicit delay actions. We study two standard timing interpretations, digital-time (Section 4) and real-time (Section 5), which are similar to the integer-clock and real (dense) time interpretations in timed automata [23]. For each setting, we devise tabular Q-learning algorithms on the product MDP obtained by composing the environment with the TRM and its clock valuations.

In the digital case, the product construction is straightforward: integer clock valuations are directly included in the MDP state space. In the dense-time case, we consider two approaches: (i) time discretization of continuous delays, and (ii) a corner-point abstraction based on region abstraction of timed automata, which encourages agents to pick delays as close as possible to integer values.

We further incorporate heuristics from the reward machine literature [24, Sec. 3.3], counterfactual-imagining, where we propose alternative wait times to the agent at the decision points.

With these abstractions and heuristics, our algorithms can optimise rewards based on satisfaction of timing constraints. We demonstrate this in Figure 1c for our running example under both digital and real-time interpretations. Notably, standard reward machines (without delay actions) cannot enforce timing constraints and therefore miss higher rewards that depend on precise timing, whereas TRMs can enable learning these.

Empirically, across standard RL benchmarks, TRMs improve performance on time-sensitive tasks and reveal clear differences between the product constructions for digital and real-time. In scenarios requiring substantial delays, the corner-point abstraction often yields better reward returns. Moreover, we also observe consistent gains from our counterfactual-imagining heuristics.

1.1 Related Work

We begin by surveying the most relevant work: RL with timed specifications, RL with non-Markovian specifications, and then the use of timed automata in control and planning.

RL with Timed Specifications. To our knowledge, only a handful of works consider time-sensitive logical reward specifications for RL. Xu and Topcu [39] optimise Metric Temporal Logic (MTL) objectives by translating them into (simple) timed automata, considering only the digital-time setting. Dole et al. [16, 17] study subclasses of Duration Calculus that compile to variants of

(a) Taxi Domain

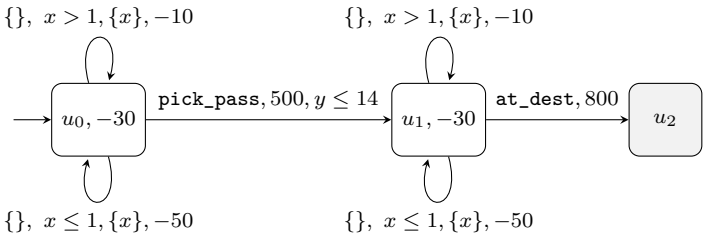

(b) TRM example

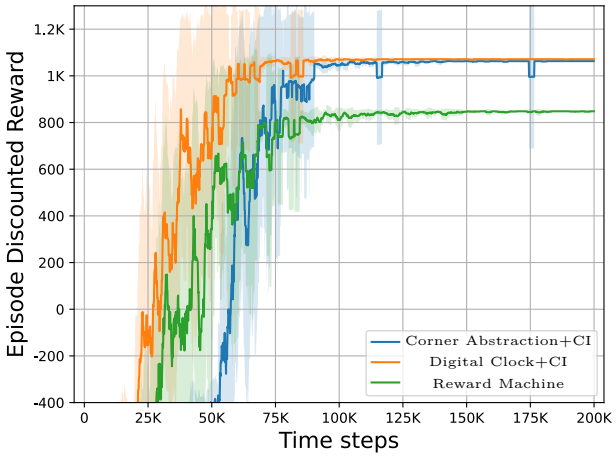

(c) Reward comparison for presented RL algorithms

Figure 1: An illustration of TRM on Gym Taxi domain: (a) Taxi Domain example, with a passenger in location red and destination in location blue, (b)A TRM that instructs the taxi to pick up a passenger and drop her at a destination, while moving slow, and (c) Rewards obtained using digital and real-time TRM, and reward machine.

timed automata. Both lines of work rely on timed automata as monitors to maximize satisfaction of timed specifications.

In contrast to these declarative specifications, our TRM formulation gives designers fine-grained control over reward logic, for example, integrating state-based delay costs and transition-based rewards, while remaining compatible with standard Markovian rewards on MDPs.

RL with Non-Markovian Rewards. To specify non-Markovian reward specifications, the most widely used formalisms are temporal logics and finite-state machines (FSMs). Among temporal logics, there has been particular focus on Linear Temporal Logic (LTL) [12, 22, 29, 11, 34, 13]. Most of these approaches typically translate formulas into FSMs that guide learning.

FSMs are central to non-Markovian RL due to their compositional structure. Reward machines (RMs) [26, 27] provide a general means of defining rewards in the FSM structure. Reward machines have been extended widely with extensions for stochastic transitions [14], ω-regular properties [21], interpreted in partial observability [28], multi-agent settings [32] and continuous-time MDP [18, 19].

Our work builds on this line and, to our knowledge, we are the first to introduce a extension of reward machines involving timing constraints.

Timed Automata in Control and Planning. Timed automata [2] are a well-established formalism for modeling and verifying systems with time-dependent behavior [10, 31]. Quantitative variants of timed automata, such as priced timed automata [5] and weighted timed automata [3], which are extensions with costs or rewards to states and transitions, have been used in strategy synthesis [4, 15] and planning [7, 8, 36].

In contrast to these approaches, which typically assume access to the underlying (MDP or game) environment, our setting is model-free: strategies must be synthesized solely via sampling the environment, without knowledge of the underlying transition graph.

2 Preliminaries and Background

2.1 Markov Decision Process

A *Markov Decision Process* (MDP) [35] is a tuple $\mathcal{M} = (S, A, T, R, \gamma)$, where S is a finite set of states, A is a finite set of actions, $T : S \times A \times S \to [0, 1]$ is the transition function that defines the probability of transitioning from state s to state s' given action a, $R : S \times A \times S \to \mathbb{R}$ is the reward function that defines the immediate reward received after taking action a in state s, and $\gamma \in [0, 1)$ is the discount factor.

Often, a labeling function is augmented in the definition of an MDP to capture key features of the system. Formally, a *labeled MDP* is a tuple $\mathcal{M} = (S, A, T, R, \gamma, \mathrm{AP}, L)$, where $L : S \times A \times S \to 2^{\mathrm{AP}}$ is a labeling function that maps each state-action-next state triplet to a set of propositions AP that hold true in that context.

A *policy* for an MDP is a mapping $\pi : (S \times A)^* S \to \Delta(A)$ that defines the distribution over actions for a given history of states and actions. For Markovian rewards, it is sufficient to consider deterministic and positional policies $\pi : S \to A$.

The expected cumulative reward for a policy π is defined as the sum of the immediate rewards received over time, discounted by the factor γ. For a policy π, it is defined as:

$$V^{\pi}(s) = \mathbb{E}_{\pi}\left[\sum_{t=0}^{\infty} \gamma^t R(s_t, a_t) \mid s_0 = s\right]$$

where s_t is the state at time t, a_t is the action taken at time t.

2.2 Reinforcement Learning with Q-learning

Reinforcement learning (RL) learns policies that maximize discounted reward in MDPs. In model-free RL, the agent samples the environment without explicit transition or reward models. Q-learning, a standard model-free method, learns the optimal action-value function $Q : S \times A \to \mathbb{R}$, the expected return of taking a in s and then following the optimal policy. The Q-learning update rule is given by:

$$Q(s,a) \leftarrow Q(s,a) + \alpha \left(R(s,a) + \gamma \max_{a'} Q(s',a') - Q(s,a) \right)$$

where α is the learning rate, $R(s,a)$ is the immediate reward received after taking action a in state s, and s' is the next state reached after taking action a in state s.

3 Problem formulation

We first introduce the Timed Reward Machines, the non-Markovian reward structure specification that we use to specify the reward structure in our RL problem.

3.1 Timed Reward Machine (TRM)

We extend classical timed automata with reward functions for the RL setting. For the reward machine formalism, we follow Toro Icarte et al. [26]. In our formalism, reward machines are augmented with a set of *clocks* X which can assume values in time domain $\mathbb{T}$. We consider two different time settings: (1) a digital-time setting, where $\mathbb{T} = \mathbb{N}$; and (2) a real-time setting, where $\mathbb{T} = \mathbb{R}_{\geq 0}$.

A *guard* is a conjunction of constraints of the form $\phi := x \bowtie c$, where $x \in X$ is a clock, $\bowtie \in \{<, \leq, =, \geq, >\}$ is a comparison operator, and $c \in \mathbb{N}$ is a non-negative constant. We denote the set of all guards over X by $\Phi(X)$. Given a set of clocks X, high-level features or propositions AP, a *timed reward machine* (TRM) is a finite state machine defined as a tuple $A = (U, u_0, F, \Delta_u, \Delta_r)$, where:

- U is a finite set of states,
- $u_0 \in U$ is the initial state,
- F is a set of terminal states,
- $\Delta_u \subseteq U \times 2^{\mathrm{AP}} \times \Phi(X) \times 2^X \times (U \cup F)$ is the transition relation defining the next state given the current state, active propositions in the current state, a guard over clocks, and the clocks to reset. We denote a transition using θ.
- $\Delta_r = \Delta_r^u \cup \Delta_r^\theta$, where $\Delta_r^u : U \to [S \to \mathbb{R}]$ is the state-based reward function and $\Delta_r^\theta : \Delta_u \to [S \times A \times S \to \mathbb{R}]$ is the transition-based reward function.

It is similar in spirit to priced timed automata [9], but it is customised for reinforcement learning, allowing for general (Markovian) reward functions in both states and transitions. In our formalism, one can think of negative rewards as costs.

A timed word $w = (d_0, l_0)(d_1, l_1) \ldots (d_n, l_n) \in (\mathbb{T} \times 2^{\mathrm{AP}})^*$ is a sequence in which $d_i \in \mathbb{T}$ is a time delay at position i and $l_i \in 2^{\mathrm{AP}}$ is the set of propositions observed after that delay at position i. A *run* $\mathcal{A}^w$ of a timed reward machine $\mathcal{A}$ on w is a sequence $(u_0, v_0) \xrightarrow{d_0,\theta_0,r_0} (u_1, v_1) \xrightarrow{d_1,\theta_1,r_1}$

$\ldots \xrightarrow{d_n,\theta_n,r_n} (u_{n+1}, v_{n+1})$, where, for each i, $u_i \in U \cup F$ is the state of the TRM, $v_i \in \mathbb{T}^{|X|}$ is the clock valuation, r_i is the reward function, and θ_i is the transition at that position. The above run satisfies the following conditions:

- u_0 is the initial state, $v_0(x) = 0$ for all $x \in X$.
- let $\theta_i = (u_i, l_i, \phi_i, \rho_i, u_{i+1}) \in \Delta_u$, then the clock valuations satisfy the following condition: $v_i + d_i$ satisfies the guard ϕ_i, and $v_{i+1} = [\rho_i](v_i + d_i)$, where $[\rho_i]$ is the reset function that resets the clocks in ρ_i to 0 and keeps the others unchanged.
- $r_i[0] = \Delta_r^\theta(\theta_i)$ and $r_i[1] = \Delta_r^u(u_i)$ are the transition-based and state-based reward functions at position i, respectively.

A TRM $\mathcal{A}$ is *deterministic* if for every state $u \in U$, every set of propositions $l \in 2^{\mathrm{AP}}$, and every pair of guards $\phi_1, \phi_2 \in \Phi(X)$ such that $(u, l, \phi_1, \rho, u') \in \Delta_u$ and $(u, l, \phi_2, \rho', u'') \in \Delta_u$, it holds that $\phi_1 \cap \phi_2 = \emptyset$. As is a common assumption in the literature on reward machines [26], we only consider deterministic TRMs.

3.2 Interpretation of TRM on MDP

We model the environment as an MDP $\mathcal{M} = (S, A', T, \gamma, L, \mathrm{AP})$, which extends the standard labeled MDP definition by including timing delays in action space: $A' = \mathbb{T} \times A$.

In our framework, the agent has the option to either act immediately or wait for a chosen amount of time before taking the next action. This waiting period is referred to as a *delay* and is selected by the agent. As a result, the agent's trajectory takes the form of a sequence $\zeta = s_0 \cdot (d_0, a_0) \cdot s_1 \cdot (d_1, a_1) \cdots (d_n, a_n) \cdot s_{n+1} \in (S \times (\mathbb{T} \times A))^* \times S$, where $s_i \in S$ is the MDP state, $d_i \in \mathbb{T}$ is the delay chosen, and $a_i \in A$ is the action taken. Since RL algorithms operate on sampled finite trajectories, this paper considers only finite trajectories obtained by bounding the maximum horizon.

A trajectory ζ induces a timed word $w^\zeta = (d_0 + 1, L(s_0, a_0, s_1)) \ldots (d_n + 1, L(s_n, a_n, s_{n+1}))$, which serves as input to the timed reward machine (TRM) $\mathcal{A}$. The offset of $+1$ in the delays accounts for the assumption that actions are executed after the specified delay. This definition aligns with the reward machines based RL settings [24]; in particular, setting all delays $d_i = 0$ yields the standard untimed word over propositions.

On this timed word w^ζ, the TRM $\mathcal{A}$ produces a run $\mathcal{A}^\zeta : (u_0, v_0) \xrightarrow{d_0+1,\theta_0,r_0} (u_1, v_1) \xrightarrow{d_1+1,\theta_1,r_1} \ldots \xrightarrow{d_n+1,\theta_n,r_n} (u_{n+1}, v_{n+1})$. We now define the discounted cumulative reward for a trajectory ζ. This definition follows the standard treatment of discounting in decision processes with sojourn times, as presented in [33, Equation 11.3.1].

Following that framework, each decision point occurring at time t_i contributes a discounted reward of $\gamma^{t_i} \cdot R_i$ to the total return, where R_i denotes the total reward accumulated during the transition from state s_i to s_{i+1} after taking action a_i. The reward R_i consists of two parts: the lumpsum reward $r_i^\theta(s_i, a_i, s_{i+1})$ obtained from the transition θ in $\mathcal{A}$ and the state-based reward $r_i^u(s_i)$ obtained from the state u in $\mathcal{A}$, accrued over the interval $[t_i, t_{i+1}]$. Formally, the total discounted cumulative reward is defined as:

$$G^\zeta = \sum_{i=0}^{n} \gamma^{t_i} \cdot [r_i^\theta(s_i, a_i, s_{i+1}) + r_i^u(s_i)], \text{where} \tag{1}$$

- $t_i = \sum_{j=0}^{i-1}(d_j + 1)$ for $i > 1$, $t_0 = 0$.

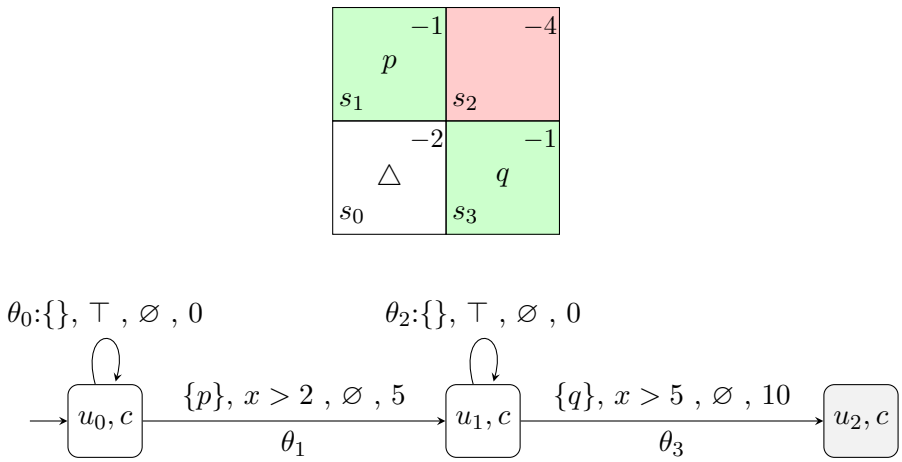

Figure 2: Environment (above) along with TRM objective (below). The cost function c is depicted in the top right corner of each state.

- $r_i^\theta = \Delta_r^\theta(\theta_i)$ is the transition-based reward at point i.
- $r_i^u = \begin{cases} \sum_{t=0}^{d_i-1} \gamma^t \Delta_r^u(u_i) = \frac{1-\gamma^d}{1-\gamma} \Delta_r^u(u_i) & \text{for } \mathbb{T} = \mathbb{N}, \\ \int_0^{d_i} \gamma^t \Delta_r^u(u_i)\, dt = \frac{1-\gamma^d}{-\ln(\gamma)} \Delta_r^u(u_i) & \text{for } \mathbb{T} = \mathbb{R}_{\geq 0} \end{cases}$
  is the state-based reward at point i.

We treat the calculation of the state-based reward r_i^u differently for the digital and real-time settings, following standard interpretations [33]. In the digital time setting, the state-based reward is accumulated at each time step during the delay period, while in the real-time setting, it is integrated over the delay interval.

Illustrative Example. To explain the above definitions, we consider the example in Figure 2 that depicts a small environment with two features, p and q, which denote moving into states s_1 and s_3, respectively. Starting at s_0, the TRM objective $\mathcal{A}$ requires the agent first to observe p and then q, while satisfying simple clock constraints.

We illustrate two trajectories, ζ_1 and ζ_2, for this example in Figure 3. The figure also summarises, for each trajectory, the induced timed words, the TRM runs, and the resulting discounted returns. Both trajectories use the same environment actions but differ in their delay choices, which leads to different behaviour under the TRM. For instance, ζ_1 waits in a "good" state s_1, whereas ζ_2 waits in a "bad" state s_2, incurring a higher cost. Consequently, in the digital-time setting with $\gamma = 0.9$, ζ_1 attains a higher discounted return ($G^{\zeta_1} \approx 6.4$) than ζ_2 ($G^{\zeta_2} \approx 5.1$). The exact ordering holds in real-time with the same delays (≈ 6.6 vs. ≈ 5.4), with the values differing due to accumulating rewards over continuous time.

Properties of TRM. We now make some observations about the trajectories and the rewards obtained from TRMs. Similar to classical timed automata, in timed reward machines, a trajectory can, in principle, induce arbitrarily large clock values and delays. However, to reason about the expected cumulative reward, one can bound the clock values and delays. As is typically done in classical timed automata, we rely on the maximum constant M appearing in the guards of the TRM $\mathcal{A}$.

We define valuations and delays bounded by the constant M as follows: $\overline{v}[x] = v[x]$ if $v[x] \leq M$ else $\overline{v}[x] = \infty$ for all $x \in X$, where ∞ denotes the clock value exceeds M. Note that ∞ will

Trajectory ζ_1

Trajectory: $\zeta_1 = s_0 \cdot (2,\uparrow) \cdot s_1 \cdot (1,\rightarrow)\, s_2 \cdot (0,\downarrow) \cdot s_3$

Timed word: $w^{\zeta_1} = (2{+}1, \{p\})(1{+}1, \emptyset)(0{+}1, \{q\})$

TRM run: $\mathcal{A}^{\zeta_1} = (u_0, [0]) \xrightarrow{3,\theta_1,(5,-2)} (u_1, [3]) \xrightarrow{2,\theta_2,(0,-1)} (u_1, [5]) \xrightarrow{1,\theta_3,(10,-4)} (u_2, [6])$

Digital-time: $G^{\zeta_1} = \big[5 + (-2)(1+\gamma^1)\big] + \gamma^3[0 + (-1)] + \gamma^5[10 + 0] \approx 6.4$

Real-time: $G^{\zeta_1} = \big[5 + (-2)\int_0^2 \gamma^t dt\big] + \gamma^3\big[0 + (-1)\int_0^1 \gamma^t dt\big] + \gamma^5[10 + 0] \approx 6.6$

Trajectory ζ_2

Trajectory: $\zeta_2 = s_0 \cdot (2,\uparrow) \cdot s_1 \cdot (0,\rightarrow)\, s_2 \cdot (1,\downarrow) \cdot s_3$

Timed word: $w^{\zeta_2} = (2{+}1, \{p\})(0{+}1, \emptyset)(1{+}1, \{q\})$

TRM run: $\mathcal{A}^{\zeta_2} = (u_0, [0]) \xrightarrow{3,\theta_1,(5,-2)} (u_1, [3]) \xrightarrow{1,\theta_2,(0,-1)} (u_1, [4]) \xrightarrow{2,\theta_3,(10,-4)} (u_2, [6])$

Digital-time: $G^{\zeta_2} = \big[5 + (-2)(1+\gamma^1)\big] + \gamma^3[0 + 0] + \gamma^4[10 + (-4)] \approx 5.1$

Real-time: $G^{\zeta_2} = \big[5 + (-2)\int_0^2 \gamma^t dt\big] + \gamma^3[0 + 0] + \gamma^4\big[10 + (-4)\int_0^1 \gamma^t dt\big] \approx 5.4$

Figure 3: Trajectories ζ_1 and ζ_2 with induced words, TRM runs, and discounted rewards for digital and real-time settings ($\gamma = 0.9$).

follow the usual comparison semantics, e.g., $\infty > 2$ is true, while $\infty \leq 3$ is false. We also define bounded delays as $\overline{d} = d$ if $d < M$ else $\overline{d} = M$.

We extend this definition to trajectories: for a trajectory $\zeta = s_0 \cdot (d_0, a_0) \cdots (d_n, a_n) \cdot s_{n+1}$, we define a delay-bounded trajectory $\overline{\zeta} = s_0 \cdot (\overline{d}_0, a_0) \cdots (\overline{d}_n, a_n) \cdot s_{n+1}$. We can show that the delay-bounded trajectory induces a similar run in a TRM $\mathcal{A}$ to the original trajectory ζ, as stated below. The proof of this follows from the fact that any clock value $v[x]$ beyond M has the same behavior with any guards on x.

Lemma 1. *Let $\zeta = s_0 \cdot (d_0, a_0) \cdots (d_n, a_n) \cdot s_{n+1}$ be a trajectory and $\overline{\zeta} = s_0 \cdot (\overline{d}_0, a_0) \cdots (\overline{d}_n, a_n) \cdot s_{n+1}$ be its delay-bounded trajectory. Also, let $\mathcal{A}^{\zeta} : (u_0, v_0) \xrightarrow{d_0+1,\theta_0,r_0} \ldots \xrightarrow{d_n+1,\theta_n,r_n} (u_{n+1}, v_{n+1})$ be the run of $\mathcal{A}$ on ζ. Then, the following holds: $\overline{\zeta}$ has run $\mathcal{A}^{\overline{\zeta}} : (u_0, \overline{v}_0) \xrightarrow{\overline{d}_0,\theta_0,\overline{r}_0} \ldots \xrightarrow{\overline{d}_n,\theta_n,\overline{r}_n} (u_{n+1}, \overline{v}_{n+1})$ where the u_i's, and θ_i's remain the same as in $\mathcal{A}^{\zeta}$.*

Proof. The proof follows from the fact that any clock value $v[x]$ beyond M has the same behavior with any guards on x. Formally, let us, w.l.o.g., consider d_i to be the first delay in ζ such that $d_i \geq M$. Let ϕ_i be the guard of transition θ_i and $v_i + d_i + 1 \models \phi_i$. Then, we have $v_i + \overline{d}_i + 1 \models \phi_i$ since constants appearing ϕ_i are bounded by M. □

While the above lemma shows that the delay-bounded trajectory $\overline{\zeta}$ induces a similar run in the TRM $\mathcal{A}$ as the original trajectory ζ, it does not guarantee that the discounted rewards $G^{\overline{\zeta}}$ and G^{ζ} are the same. However, under certain reasonable conditions, bounding the delays can improve the obtained discounted reward, which we will consider in this paper. These include inducing costs for delaying in states rather than rewarding, and providing a high terminal reward for completing all tasks.

To formalise this, we assume that the state–reward function always has negative values, i.e., $\Delta_r(u) < 0$for every $u \in \mathcal{A}$. Also, we search for "good" trajectories ζ for which $G_i^\zeta > 0$ for all decision points i, G_i^ζ being the discounted return from i onward. Trajectories like ζ can occur, for example, when terminal rewards along ζ are sufficiently large. For these assumptions, we now state the following lemma, which shows that delay-bounded trajectories can achieve a better discounted reward. Intuitively, the result follows from the fact that shorter delays lower state costs and also reduce the discounting applied to terminal rewards.

Lemma 2. *Let ζ be a trajectory and $\overline{\zeta}$ be its delay-bounded trajectory. We assume that corresponding TRM $\mathcal{A}$ and trajectory ζ satisfy the following conditions: (1) the state-based rewards are always negative, i.e., $\Delta_r^u(u) < 0$ for all $u \in U$; and (2) discounted reward $G_i^\zeta > 0$ is positive for every decision time $0 \leq i \leq n$. Then, $G^{\overline{\zeta}} \geq G^\zeta$.*

Proof. We demonstrate for the digital case (as it is similar to the real-time case), using backward induction on the length i of the trajectory. As the hypothesis, we consider that $G_i^{\overline{\zeta}} \geq G_i^\zeta$ for every $i > k$. For the decision point k, we show $(G_k^{\overline{\zeta}} = R_k^{\overline{\zeta}} + \gamma^{\overline{d}+1} G_{k+1}^{\overline{\zeta}}) \geq (G_k^\zeta = R_k^\zeta + \gamma^{d+1} G_{k+1}^\zeta)$. Firstly, the reward $R_k^{\overline{\zeta}} > R_k^\zeta$ is higher for trajectory since state rewards accrue less cost: $\frac{1-\gamma^d}{1-\gamma}\Delta_r^u(u_k) < \frac{1-\gamma^{\overline{d}}}{1-\gamma}\Delta_r^u(u_k)$. Secondly, the $\gamma^{\overline{d}+1} G_k^{\overline{\zeta}} \geq \gamma^{d+1} G_k^{\overline{\zeta}} \geq \gamma^{d+1} G_k^\zeta$. □

Based on the assumptions of the above lemma, we can therefore bound the delay space to $\mathbb{D} = \mathbb{T} \cap [0, M]$. In our setting, policies can be defined as $\pi : (S \times \mathbb{D} \times A)^* S \to \mathbb{D} \times A$, which maps a trajectory to a bounded delay and an action. We call such policies *delay-discounted* policies, since the reward functions defined in Equation (1) incorporate the discount factor to delays as well.

The expected cumulative reward of a policy π is defined as the expected discounted sum of rewards over all possible trajectories that follow π, starting from a state s: $V^\pi(s) = \mathbb{E}_{\zeta \sim \pi}[G^\zeta \mid \zeta[0] = s]$.

Problem 1 (Optimal Policy Synthesis for TRMs)**.** *Given a TRM $\mathcal{A}$ and a MDP M, find a delay-discounted policy π^* that maximizes the expected cumulative reward, i.e., $\pi^* = \arg\max_\pi V^\pi(s)$.*

In the following sections, we propose algorithms for Problem 1, both in the digital and the real-time settings.

4 The Digital Clock Setting

Cross-product space. The most important aspect of our approach is the construction of a cross-product between the underlying MDP M and the TRM $\mathcal{A}$.

The cross-product MDP $\mathcal{M}^\otimes = \mathcal{M} \otimes \mathcal{A}$ is similar to what is done for classical reward machines, except that one needs to keep track of the clock values as well. For this, we again consider the maximum constant M appearing in the guards of clock $x \in X$ of $\mathcal{A}$ and use the symbol ∞ for clock values that go beyond M.

The cross product $(S^\otimes, A^\otimes, T^\otimes, R^\otimes)$ is defined below, where:

- $S^\otimes = S \times U \times V$, where S is the set of states of the MDP and U is the set of states of the TRM, and $V = (\{0, \ldots, M\} \cup \{\infty\})^{|X|}$ is the set of bounded clock valuations.
- $A^\otimes = \mathbb{D} \times A$ is the set of actions.

- $T^{\otimes} : S^{\otimes} \times A^{\otimes} \times S^{\otimes} \to [0,1]$ and $R^{\otimes} : S^{\otimes} \times A^{\otimes} \times S^{\otimes} \to \mathbb{R}$ are the transition function and the reward function, respectively, defined as follows:

$$T^{\otimes}((s,u,v),(d,a),(s',u',v')) = T(s,a,s'), \text{and}$$
$$R^{\otimes}((s,u,v),(d,a),(s',u',v')) = r^u(s) + r^{\theta}(s,a,s'), \text{if}$$
$$\exists \theta = (u, L(s,a,s'), \phi, \rho, u'), \text{s.t. } v + d + 1 \models \phi, v' = [\rho](v+d+1),$$

where for all $x \in X$, $(v+d+1)[x] = v[x]+d+1$ if $v[x]+d+1 \leq M$, otherwise ∞; $r^u = \frac{1-\gamma^d}{1-\gamma}\Delta_r^u(u)$, and $r^{\theta} = \Delta_r^{\theta}(\theta)$.

Theorem 1. *Optimal positional deterministic delay-discounted policy exists for the cross product MDP $\mathcal{M}^{\otimes}$.*

The proof holds, following standard results in MDPs [33], because the cross product $\mathcal{M}^{\otimes}$ has a finite state and action space.

Q-learning on cross-product space. We adapt Q-learning to the cross-product space by modifying the Q-value updates as follows:

$$Q((s,u,v),(d,a)) \leftarrow Q((s,u,v),(d,a)) + \alpha\left([R + \gamma^{(d+1)} \max_{(d',a')} Q((s',u',v'),(d',a'))] - Q((s,u,v),(d,a))\right),$$

where R is the reward returned by the TRM $\mathcal{A}$ for the transition from (s,u,v) to (s',u',v') on choosing delay of d and action a.

The convergence follows from standard results [38], since $\mathcal{M}^{\otimes}$ is a valid finite MDP with probabilities $p((s',u',v')|(s,u,v),(d,a)) = p(s'|s,a)$.

Theorem 2. *Q-learning on the cross-product $\mathcal{M}^{\otimes}$ converges to an optimal policy under standard assumptions: every state $(s,u,v) \in S^{\otimes}$ and action $(d,a) \in A^{\otimes}$ is visited infinitely often; and the learning rate α_t is decreased over time such that $\sum_{t=0}^{\infty} \alpha_t = \infty$ and $\sum_{t=0}^{\infty} \alpha_t^2 < \infty$.*

4.1 Counterfactual Imagining for Delays

Adding delay actions substantially enlarges the action space, so we use *counterfactual imagining* to explore time alternatives efficiently.

During the Q-learning process, given a realised transition $\langle (s,\bar{u},\bar{v}),(d,a),r,(s',u',v')\rangle$ in the product MDP , we synthesize counterfactual experiences by varying the TRM states, clock valuations, and delays:

$$\langle (s,u,v),\ (\bar{d},a),\ \bar{r},\ (s',\bar{u}',\bar{v}')\rangle,$$

where $(\bar{u},\bar{v}) \xrightarrow{\bar{d},\theta,\bar{r}} (\bar{u}',\bar{v}')$ is a single step based on TRM.

Varying valuations $\bar{v}$ and delays $\bar{d}$ over all possibilities requires adding several alternatives due to potentially large clock range $\{0,\ldots,M\}$. To keep the number of counterfactuals manageable, we consider adding only reasonable alternatives for valuations and delays. First, we only consider valuations $\bar{v}$ that are close to the realized valuation v, i.e., $\|\bar{v} - v\|_{\infty} \leq r_{crm}$ for a fixed radius r_{crm} (typically less than 5). Second, we consider delays $\bar{d}$ that enable satisfaction of guards in the alternative TRM state $\bar{u}$ and clock valuation $\bar{v}$. In particular, we add delays $\bar{d}$ corresponding to all transitions $\theta = (\bar{u}, L(s,a,s'), \phi, \rho, \bar{u}')$ such that $\bar{v} + \bar{d} + 1 \models \phi$.

In contrast, for (untimed) reward machines [24], counterfactuals vary only the RM state $\bar{u}$, without varying clocks or delays.

5 The Real-time Clock Setting

In the continuous-time case, clock values and delay actions can be real-valued, and delays can be chosen from the continuous range $[0, M]$, enabling more precise timing of actions. This allows for more possible policies, often leading to better rewards.

For instance, the example in Figure 4 admits no positive-valued policy in the digital-clock setting, while the real-time setting allows for suitable positive-valued policies. In the real-time setting, the following trajectory: $\zeta_1 = s_0 \cdot (0.1, \rightarrow) \cdot s_1 \cdot (0, \rightarrow) \cdot s_2$ can achieve a discounted reward of $[5 + (-1)(1 - \gamma^{0.1})/-\ln(\gamma)] + \gamma^{1.1}[7] \approx 11.13$ for $\gamma = 0.9$. In contrast, similar trajectories $\zeta_2 = s_0 \cdot (0, \rightarrow) \cdot s_1 \cdot (0, \rightarrow) \cdot s_2$ and $\zeta_3 = s_0 \cdot (1, \rightarrow) \cdot s_1 \cdot (0, \rightarrow) \cdot s_2$ will achieve discounted rewards of $-10+\gamma^1[7] \approx -3.7$ and $[5+(-1)(1-\gamma^1)/(1-\gamma)]+\gamma^2[-10] \approx -4.1$, respectively, in the digital-clock setting.

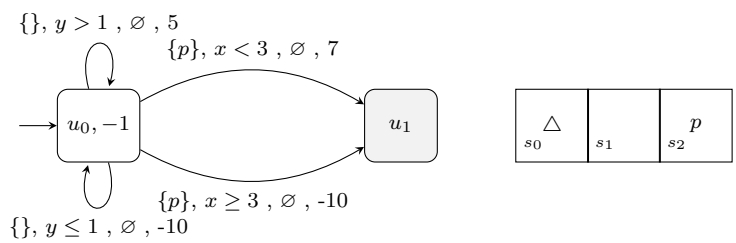

Figure 4: TRM (on the left) and MDP (on the right) illustrating agent behavior in the real-time setting.

Moreover, in contrast to the digital-time case, in the real-time setting, optimal policies may not exist, as stated below

Theorem 3. *Optimal delay-discounted policy may not exist in the real-time setting.*

The above result can be seen from Figure 4. The best sequence $(d, \rightarrow)(0, \rightarrow)$, $0 < d < 1$, yields return $G^\zeta = [5 + \frac{(1-\gamma^d)}{-\ln(\gamma)}(-1)] + \gamma^{(1+d)}[7]$. This will achieve a supremum of 11.3 as $d \rightarrow 0^+$, but this is unattainable since $d = 0$ violates the guard.

We will therefore focus on learning "near-optimal" policies. To this end, we consider various (discrete) abstractions of continuous-time, enabling us to exploit tabular RL algorithms.

Uniform Discretization of Continuous Time. A naive approach to approximating real-time is to use a uniform discretization. This would mean partitioning the time domain using a step size $0 < \frac{1}{\kappa} < 1$, $\kappa > 1 \in \mathbb{N}$. In this setting, the clock valuations would be the set $V_\kappa = \{v \in ([0, M] \cup \{\infty\})^{|X|} \mid v[x] = c/\kappa \text{ or } v[x] = \infty \text{ for } c = 0, \ldots, M \cdot \kappa, \text{ for all } x \in X\}$ and the delay action space $\mathbb{D}_\kappa = \{c/\kappa \in [0, M] \mid c = 0, \ldots, M \cdot \kappa\}$.

The cross-product MDP $\mathcal{M}^\otimes$ can then be constructed as in the digital-clock case, except that the action space and state space are defined as above. One can therefore apply the Q-learning algorithm developed in Section 4 and achieve similar convergence guarantees on the considered cross-product MDP.

To achieve better approximations of the optimal value using uniform discretization, one would require choosing a larger partition κ. However, the size of the valuation space $|V_\kappa|$ and $|\mathbb{D}_\kappa|$ grows with κ, specifically $|V_\kappa| = (M \cdot \kappa + 1)^{|X|}$ and $|\mathbb{D}_\kappa| = M \cdot \kappa + 1$. This leads to a significant increase in the state and action space of the cross-product MDP, hindering the scalability of this approach.

5.1 Corner-Point Abstraction based on Regions

To address the challenges arising from discretizing real-time, several approaches have been proposed that construct principled abstractions of clock valuations for timed state machines [1].

In this work, we will adapt the corner-point abstraction formulation that is based on the region abstraction [1]. While this has already been used in the context of priced timed automata [7, 8], we adapt it to interpret TRMs over MDPs for discounted rewards.

The key idea of regions is to partition the infinite set of clock valuations into finitely many equivalence classes that behave identically with respect to guards. Region corners are the nearby integral boundary points; choosing delays near such corners often yields a higher reward (as in Figure 4).

To formally introduce the corner-point abstraction, we briefly recall the region abstraction and then define its corner points. Given a set of clocks X and a max-constant M, a *region* is a tuple $(h, [X_0, \ldots, X_p])$, where $h : X \to \{0, \ldots, M\}$, and $(X_i)_{i=0}^{p}$ is a partition of X such that for all $i > 0$, $X_i \neq \emptyset$ and $h(x) = M$ implies $x \in X_0$. A valuation v is in a region if the following conditions hold:

- for all $x \in X$, $\lfloor v(x) \rfloor = h(x)$,
- for all $x \in X$, $x \in X_0$ iff $\{v(x)\} = 0$ (i.e., $v(x) = h(x)$), and
- for all $x, y \in X$, $\{v(x)\} \leq \{v(y)\}$ iff $x \in X_i$, $y \in X_j$, $i \leq j$,

where $\lfloor c \rfloor$ and $\{c\}$ denote the integer and fractional parts of c, respectively. For example, the valuation v with $v(x) = 1.2$, $v(y) = 0.5$ lies in the region $R = (\{x : 1, y : 0\}, [\{\}, \{x\}, \{y\}])$. Two valuations $v, \overline{v}$ are *region-equivalent*, denoted $v \sim \overline{v}$, if they belong to the same region. For a valuation v, $[v]$ denotes the region to which it belongs.

A corner point is a valuation $v \in \{0, \ldots, M\}^{|X|}$ with integral values for each clock. A corner point of a region R belongs to the (topological) closure of R. For example, the corner points of the example region above are $(1, 0)$, $(1, 1)$, and $(2, 1)$.

For a precision $\varepsilon > 0$, we define the ε-corners of a region R to be $C_\varepsilon(R) = \{v \in R \mid \forall x, v(x) \in (c - \varepsilon, c + \varepsilon)$ where c is a corner of $R\}$ the valuations close to its corners.

Given a trajectory $\zeta = s_0 \cdot (d_0, a_0) \cdots (d_n, a_n) \cdot s_{n+1}$, we define its *region-equivalent trajectories* $[\zeta]$ to be the set of all trajectories $\hat{\zeta}$ of the form $s_0 \cdot (\hat{d}_0, a_0) \cdots (\hat{d}_n, a_n) \cdot s_{n+1}$ such that for all $i \in \{0, n+1\}$, $v_i \sim \hat{v}_i$, where v_i and $\hat{v}_i$ are the valuations appearing in $\mathcal{A}^\zeta$ and $\mathcal{A}^{\hat{\zeta}}$. Given a trajectory ζ and an ε, we define *region-equivalent corner trajectories* of ζ, denoted by $C_\varepsilon(\zeta)$, as the set of trajectories $\hat{\zeta}$ such that $\hat{\zeta} \in [\zeta]$ and $\hat{v}_i \in C_\varepsilon([v_i])$ for all valuations v_i and $\hat{v}_i$ appearing in the runs $\mathcal{A}^\zeta$ and $\mathcal{A}^{\hat{\zeta}}$, respectively.

We now show that, for a trajectory ζ, moving its valuations v_i's to the corners improves the discounted reward; the proof proceeds via an induction on i, improving the reward iteratively.

Lemma 3. *For any trajectory ζ, there exists a region-equivalent corner trajectory $\hat{\zeta} \in C_\varepsilon(\zeta)$ such that $G^{\hat{\zeta}} \geq G^\zeta$.*

Proof. The proof proceeds inductively on the length of the trajectory ζ. We modify $\zeta = \hat{\zeta}_0$ in each inductive step to $\hat{\zeta}_i$ to ensure that the valuation $\hat{v}_i$ at each decision point i is in $C_\varepsilon([v_i])$. In induction step i, we assume the hypothesis that in trajectory $\hat{\zeta}_{i-1}$, for all $j < i$, $\hat{v}_j$ are in $C_\varepsilon([v_j])$, $G^{\hat{\zeta}_{i-1}} \geq G^{\hat{\zeta}_j}$. Now, we create $\hat{\zeta}_i$ from $\hat{\zeta}_{i-1}$ by modifying $\hat{d}_i$ to make $\hat{v}_i \in C_\varepsilon([v_i])$, and from decision point $i+1$ onwards $\hat{\zeta}_i$ and $\hat{\zeta}_{i-1}$ are identical. We now like to check that the reward $G^{\hat{\zeta}_i} \geq G^{\hat{\zeta}_{i-1}}$.

We consider the difference in the calculation of $G^{\hat{\zeta}_i}$ and $G^{\hat{\zeta}_{i-1}}$. For this, we note that the only difference between the two trajectories is time at the decision point i; for ζ_i we refer using t'_i and for ζ_{i-1} using t_i. We can now write the following:

$$
\begin{aligned}
G^{\hat{\zeta}_i} - G^{\hat{\zeta}_{i-1}} &= [\gamma^{t_{i-1}}(\Delta^{\theta}_{i-1} + \frac{(1-\gamma^{d'_{i-1}})}{-\ln\gamma}\Delta^{u}_{i-1}) - \gamma^{t_{i-1}}(\Delta^{\theta}_{i-1} + \frac{(1-\gamma^{d_{i-1}})}{-\ln\gamma}\Delta^{u}_{i-1})] \\
&+ [\gamma^{t'_i}(\Delta^{\theta}_{i} + \frac{(1-\gamma^{d'_{i}})}{-\ln\gamma}\Delta^{u}_{i}) - \gamma^{t_i}(\Delta^{\theta}_{i} + \frac{(1-\gamma^{d_{i}})}{-\ln\gamma}\Delta^{u}_{i})] \\
&= \frac{\Delta^{u}_{i-1}}{-\ln\gamma}[\gamma^{t_{i-1}+d_{i-1}} - \gamma^{t_{i-1}+d'_{i-1}}] + \Delta^{\theta}_{i}(\gamma^{t'_i} - \gamma^{t_i}) + \frac{\Delta^{u}_{i}}{-\ln\gamma}(\gamma^{t'_i} - \gamma^{t_i}) \\
&= \frac{\Delta^{u}_{i-1}}{-\ln\gamma}(\gamma^{t_i} - \gamma^{t'_i}) + \Delta^{\theta}_{i}(\gamma^{t'_i} - \gamma^{t_i}) + \frac{\Delta^{u}_{i}}{-\ln\gamma}(\gamma^{t'_i} - \gamma^{t_i}) \\
&= (\gamma^{t'_i} - \gamma^{t_i}) \cdot (\Delta^{\theta}_{i} + \frac{\Delta^{u}_{i}}{-\ln\gamma} - \frac{\Delta^{u}_{i-1}}{-\ln\gamma}) = (\gamma^{t'_i} - \gamma^{t_i}) \cdot K.
\end{aligned}
$$

In the above equation, the second term is constant, therefore replaced by K. Now, K could be either positive or negative, and depending on the sign of K, we can set t'_i in a way such that it lies in one of the corners of the corresponding region, and that the above quantity becomes positive. □

We now extend the definition of "region-equivalent corner sets" from trajectories to policies. Let π and $\hat{\pi}$ be deterministic positional policies such that, for each state (s, u, v) in the cross product MDP, $\pi(s, u, v) = (d, a)$ and $\hat{\pi}(s, u, v) = (d', a)$, i.e., both prescribe the same discrete action a but possibly different delays d and d'. We say that $\hat{\pi} \in C_{\varepsilon}(\pi)$ is a *region-equivalent corner policy* of π if for all (s, u, v), $d' = d$, if $v \notin C_{\varepsilon}([v])$, and $v + d' \in C_{\varepsilon}([v + d])$ otherwise.

We can extend the previous lemma for the following result:

Lemma 4. *For any delay-discounted policy π, there exists a region-equivalent corner policy π' such that $V^{\pi'}(s) \geq V^{\pi}(s)$.*

Proof. Since we have fixed a horizon, we can also perform a similar inductive construction of a policy π' from π as the previous result. Here, the proof proceeds via an induction on the depth i of the induced Markov chain $\mathcal{M}_{\pi}$ of the policy. Following a similar calculation, for a state s at the ith depth, the difference between $V^{\pi'_i}(s)$ and $V^{\pi_i}(s)$ can be written as:

$$
\sum_{\zeta \in \mathcal{M}_{\pi_{i-1}}, \hat{\zeta} \in \mathcal{M}_{\pi_i}} Pr_{\zeta \sim \mathcal{M}_{\pi}}[G^{\hat{\zeta}} - G^{\zeta}] = \sum_{\zeta, \hat{\zeta}} Pr_{\zeta \sim \mathcal{M}_{\pi}} \cdot K \cdot (\gamma^{t'_i} - \gamma^{t_i}) = K' \cdot (\gamma^{t'_i} - \gamma^{t_i}).
$$

Then, based on the sign of the constant K, we can modify the policy π_i such that t'_i is in one of the corners and the above difference is positive. □

We can therefore focus our attention to only region-equivalent corner policies. Although it significantly reduces the search space, an infinite number of such policies can still exist. To address this, we introduce a 'finite' abstraction of the cross-product MDP, where valuations correspond to the corners of the regions. We then show that this finite MDP provides a near-optimal approximation of the original real-time MDP.

Cross-product using Corner-Point Abstraction. To define the cross-product MDP in this case, we first describe how a corner configuration (R, α) of the corner-abstraction of $\mathcal{A}$, where R is a region and α is a corner point of R, evolves under elapsing time.

In this setting, the agent, in addition to a delay $d \in \mathbb{D} = \{0, \ldots, M\}$, chooses a region successor $\sigma \in \mathbb{S} = \{-2|X|, \ldots, 0, \ldots, 2|X|\}$ that assigns which region to move to associated with a corner[1].

[1]Some successors may be invalid and/or not distinct for certain types of (R, α).

Intuitively, applying a delay-successor tuple (d, σ) to a configuration (R, α) leads to a new configuration (R', α') obtained as follows: first shift both R and α by d time unit, and then choose the σth successor region associated with that corner. Formally, $(R, \alpha) \oplus (d, \sigma)$ is the new configuration (R', α') defined as: $\alpha' = \alpha + d$, $R''[h] = R[h] + d$ and R' is the σth successor region of R'' associated with α'.

To understand the above definitions, consider an example corner configuration $(R = (\{x : 1, y : 0\}, [\{x\}, \{y\}]), \alpha = (1, 0))$. This region contains valuations such as $v(x) = 1$, $v(y) = 0.1$. Applying delay, $(1, 0)$ leads to $(R_1 = (\{x : 2, y : 1\}, [\{x\}, \{y\}]), \alpha_1 = (2, 1))$, which is essentially the same region and corner pair offset by $+1$. This region contains valuations such as $v(x) = 2$, $v(y) = 1.1$. On the other hand, applying time elapse $(1, 1)$ leads to $(R_2 = (\{x : 2, y : 1\}, [\{\}, \{x\}, \{y\}]), \alpha_2 = (2, 1))$, which is the region successor of R_1 associated with the same corner α_2. This region contains valuations such as $v'(x) = 2.1$, $v'(y) = 1.2$.

We then define the cross-product MDP $\mathcal{M}^{\otimes} = (S^{\otimes}, A^{\otimes}, T^{\otimes}, R^{\otimes})$ as follows: $S^{\otimes} = S \times U \times \mathcal{R} \times \mathcal{C}$, where $\mathcal{R}$ is the set of regions of $\mathcal{A}$, and $\mathcal{C}$ is the set of corner points associated with the regions; $A^{\otimes} = \mathbb{D} \times \mathbb{S} \times A$, where $\mathbb{D} = \{0, 1, \ldots, M\}$ and $\mathbb{S} = \{-2|X|, \ldots, 0, \ldots, 2|X|\}$; and $T^{\otimes} : S^{\otimes} \times A^{\otimes} \times S^{\otimes} \to [0, 1]$ and $R^{\otimes} : S^{\otimes} \times A^{\otimes} \times S^{\otimes} \to \mathbb{R}$ are defined as follows:

$$
\begin{aligned}
T^{\otimes}((s, u, R, \alpha), (d, \sigma, a), (s', u', R', \alpha')) &= T(s, a, s'), \text{and} \\
R^{\otimes}((s, u, v), (d, \sigma, a), (s', u', v')) &= r^u(s) + r^{\theta}(s, a, s'), \text{if} \\
\exists \theta = (u, L(s, a, s'), \phi, \rho, u'), \text{s.t. } v + d + 1 &\models \phi, v' = [\rho](v + d + 1); \\
(R'', \alpha'') = (R, \alpha) \oplus (d + 1, \sigma) \text{ and } \; R'' &\models \phi, R' = [\rho](R''),
\end{aligned}
$$

where for all $x \in X$, $(v+d+1)[x] = v[x]+d+1$ if $v[x]+d+1 \leq M$, otherwise ∞; $r^u = \frac{1-\gamma^d}{-\ln(\gamma)} \Delta_r^u(u)$, and $r^{\theta} = \Delta_r^{\theta}(\theta)$.

The above operations on regions such as successor and reset are well-defined and can be computed efficiently [1].

We then show that an optimal policy in the corner-point abstraction MDP serves as a good approximation of region-equivalent corner policies in the original MDP in the real-time setting:

Theorem 4. *For every corner policy π in MDP $\mathcal{M}$ with a TRM $\mathcal{A}$, there exists a policy π' in the corner-point abstraction MDP $\mathcal{M}^{\otimes}$, such that, given any $\delta > 0$, $|V^{\pi}(s) - V^{\pi'}(s)| < \delta$.*

Proof. Consider a corner policy π in MDP $\mathcal{M}$ with a TRM $\mathcal{A}$. We now construct a corresponding policy π' in the corner-point abstraction $\mathcal{M}^{\otimes}$ as follows. For every cross-product state (s, u, v) such that $v \in C_{\varepsilon}([v])$ and $\pi(s, u, v) = (d, a)$, we define

$$\pi'((s, u, ([v], \alpha))) = ((d', \sigma), a),$$

where α is the closest corner in $(v - \varepsilon, v + \varepsilon)$, and the parameters (d', σ) satisfy:

1. $v + d \in C_{\varepsilon}(R')$ where $(R', \alpha') = ([v], \alpha) \oplus (d', \sigma)$;
2. $v + d'$ is the closest corner point of $[v + d]$, i.e., $v + d$ and $v + d'$ correspond to the same corner of their respective regions.

By construction, the offsets between the concrete and abstract valuations are bounded: $|\alpha - v| \leq \varepsilon$ and $|\alpha' - (v + d)| \leq \varepsilon$. Hence, the induced delay shift satisfies $|d' - d| \leq 2\varepsilon$. As rewards in $\mathcal{M}$ are continuous with respect to delay and clock valuations inside each region (the guards and resets unchanged), the difference in immediate reward between π and π' at any step is bounded by a Lipschitz-continuous function $f(\varepsilon)$ satisfying $f(\varepsilon) \to 0$ as $\varepsilon \to 0$.

The discount factor does not amplify this bound since $0 < \gamma^k \leq 1$ for all k. Restricting to trajectories of bounded horizon H, the total cumulative reward discrepancy satisfies $|G_\pi - G_{\pi'}| \leq H \cdot f(\varepsilon)$. Consequently, $|V_\pi(s) - V_{\pi'}(s)| \leq H \cdot f(\varepsilon)$. Choosing ε sufficiently small such that $H \cdot f(\varepsilon) < \delta$ yields the desired approximation guarantee: $|V_\pi(s) - V_{\pi'}(s)| < \delta$. □

Hence, standard Q-learning algorithms can be applied on the corner-point abstraction MDP $\mathcal{M}^\otimes$ to obtain the optimal policy, and thus this allows us to get a near-optimal policy in $\mathcal{M}$.

We also design counterfactual imagining for the corner abstraction, analogous to the digital-time setting (Section 4.1). By contrast, here we synthesize alternative corner configurations $(\bar{R}, \bar{c})$ within a bounded radius r_{crm} of the realised configuration (R, c). Moreover, we add alternative delay and successor actions whenever the resulting configuration $(\bar{R}, \bar{c}) \oplus (\bar{d}, \bar{\sigma})$ satisfies the relevant guards.

6 Evaluation

All the described algorithms were implemented in Python3[2] by extending [25]. We developed the timing extensions, including region and corner abstractions, for reward machines from scratch.

To improve learning performance, we employed several heuristics for interpreting TRMs. First, to reduce clock-valuation space V, we assigned clock-specific maximum constants M_x for $x \in X$, a standard optimisation in timed automata. Second, to reduce delay-space $\mathbb{D}$, we set the maximum delay M_d to the largest constant appearing in guards of the form $x \bowtie c$ with $\bowtie \in \{>, \geq, =\}$. This is not a restriction, as delays larger than M_d only incur additional costs and therefore do not need to be considered for optimal policies.

6.1 Experimental Results.

We address two key research questions here: RQ1: performance gains from counterfactual imagining; and RQ2: performance differences across various time interpretations.

To do so, we use standard Gym environments: (i) the *Taxi* domain (as in Figure 1a), with propositions indicating colored pick-up locations and whether the passenger is in the taxi or at the destination; and (ii) *Frozen Lake* (default 8×8), augmented with three goals (a, b, c) and ten holes (h), with action success probability 0.8 [37].

We use Q-learning with per-episode parameter decay 0.999, initial rate $\alpha_0 = 0.9$, initial exploration $\varepsilon_0 = 0.9$, initial Q-values $Q_0 = 10$, $\gamma = 0.999$ and maximum global steps of 300 K. For counterfactuals, we select the top 15 by rewards per transition. We averaged the results of each experiment over 10 independent runs.

[2]available at `https://github.com/ritamraha/Timed-Reward-Machines`

(a) Taxi domain (b) Frozen Lake

Figure 5: Gym environments used in experiments.

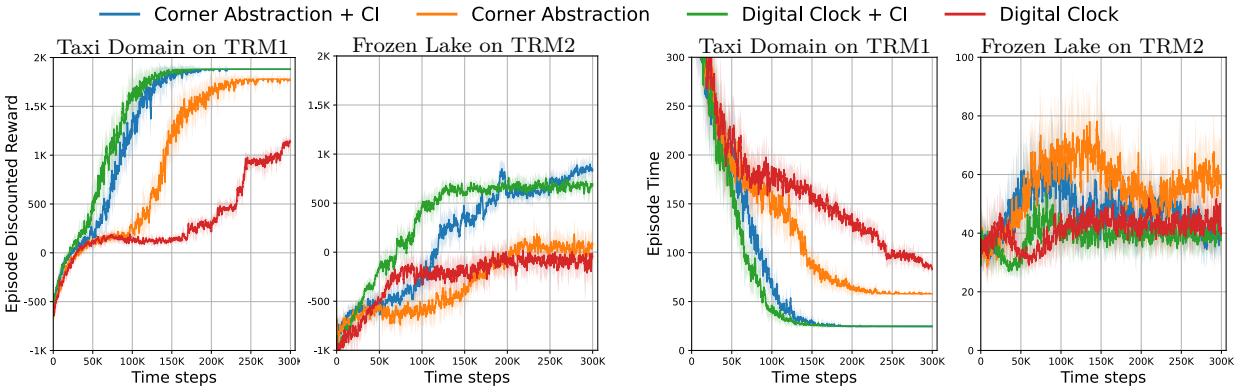

(a) Discounted reward comparison (b) Episode time comparison

Figure 6: RQ1: Performance gain for counterfactual imagining for digital and real-time settings for two environments.

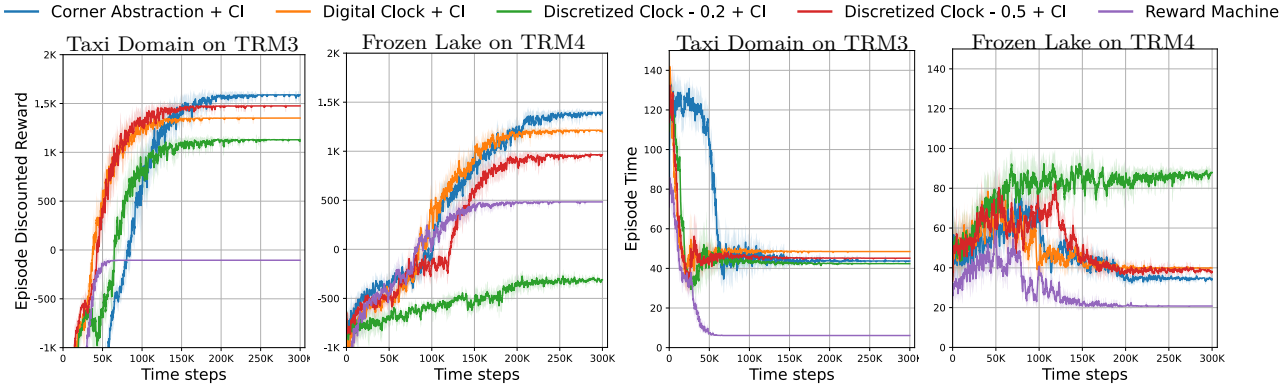

(a) Discounted reward comparison (b) Episode time comparison

Figure 7: RQ2: Performance difference for various timed interpretations

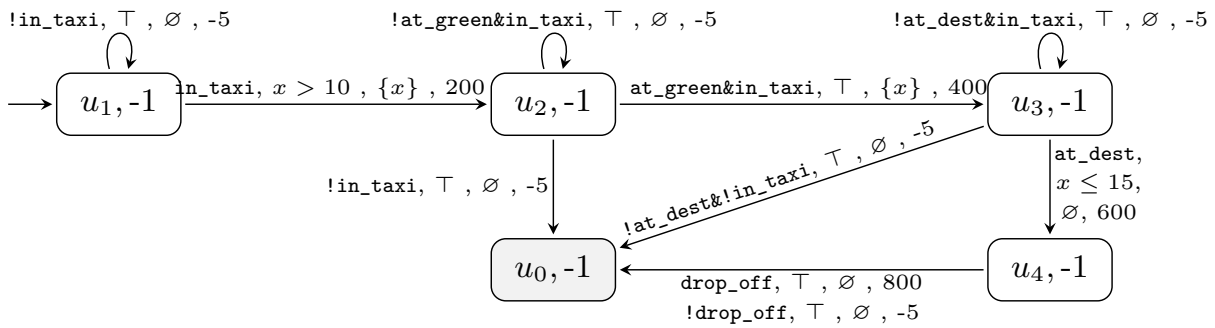

(a) TRM1 for Taxi

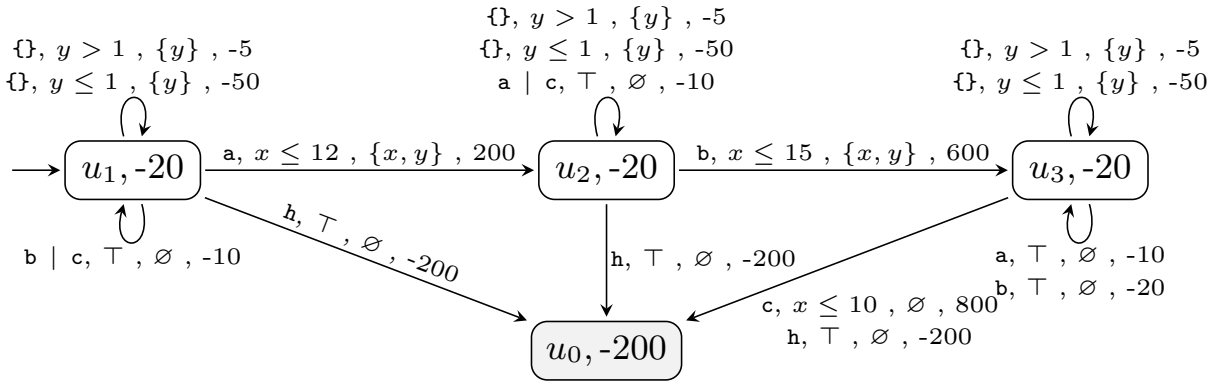

(b) TRM2 for FrozenLake

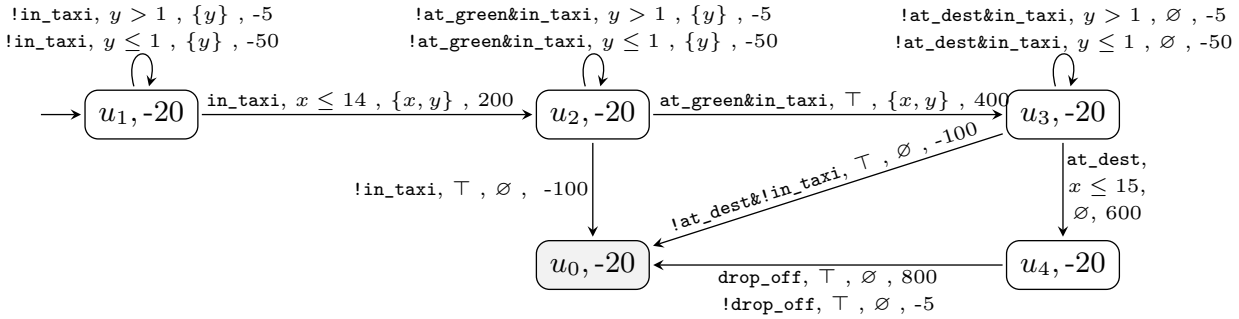

(c) TRM3 for Taxi

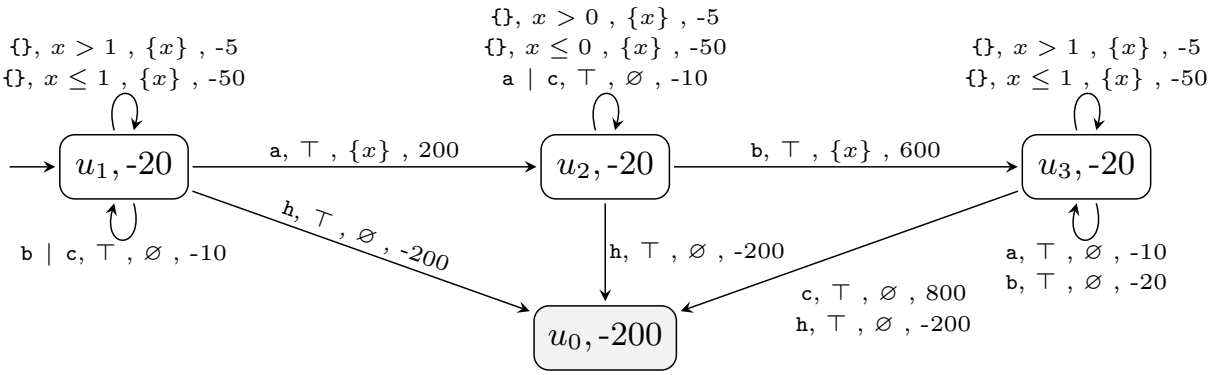

(d) TRM4 for FrozenLake

Figure 8: TRMs for Experimental Evaluations

RQ1: Performance gain for Counterfactual Reasoning

To analyze the improvement of counterfactual imagining (CI) specific to time, we only choose alternative clock valuations and delays (and not TRM states) for both the digital and the real-time settings. We demonstrate this comparison on the Taxi domain with TRM1 (Figure 8a), and on the frozen lake with TRM2 (Figure 8b). TRM1 requires the Taxi agent to pick up a passenger, visit a green location, and drop them at the destination, while satisfying several timing constraints. On the other hand, TRM2 requires the Frozen Lake agent to satisfy three objectives, a, b, c, sequentially, while avoiding falling into the holes, and it must also move slowly.

Figure 6 compares discounted returns and episode time (including delays) during Q-learning on both environments. Counterfactuals yield significantly higher returns in both digital and corner-point abstractions by enabling exploration of additional ways to satisfy timing constraints. They also significantly reduce episode time, allowing agents to complete tasks faster.

RQ2: Comparison of Timing Abstractions

We evaluate the performance of different cross-products for different time interpretations: (i) digital clock abstraction, (ii) uniform discretization with $1/\kappa \in \{0.2, 0.5\}$, (iii) corner-point abstraction, and (iv) reward machines. Note that the reward machine interpretation cannot choose delay actions, as it is not designed for timed specifications. We demonstrate this comparison on the Taxi domain with TRM3 (Figure 8c), and on the frozen lake with TRM4 (Figure 8d). The TRMs are similar to the previous experiment, with different time constraints.

Figure 7 compares discounted returns and episode time (including delays) during Q-learning on both environments. The plots in Figure 7a show that the corner-point abstraction consistently outperforms the other interpretations in terms of discounted return. This advantage arises from the ability to select delays that lie close to the guard conditions (i.e., $y > 1$), thereby enabling the agent to satisfy timing requirements precisely. While comparing the episode time, we notice that reward machines lead to the shortest episodes; however, this behavior is undesirable in this setting, as excessively completing episodes too fast violates several timing constraints.

7 Conclusion

We studied model-free RL for *Timed Reward Machines* (TRMs), a formalism that extends reward machines with explicit timing constraints. We interpreted TRMs over MDPs under digital and real-time semantics and devised abstractions for efficient learning. Our experiments with non-trivial timed specifications show that TRMs enable learning policies with delays for maximizing rewards.

This work represents a step toward improving time-sensitive reward specification in RL, with numerous avenues ahead. One can apply TRMs to continuous-time Markov models [19], which better capture rate-based timing; adapt deep continuous RL (e.g., TD3 [20]) to continuous-time; and incorporate guidance from priced zones [6] to improve exploration of TRM objectives.

Acknowledgements. This project received funding from the ERC under the European Union's Horizon 2020 research and innovation programme (grant agreement No.834115, FUN2MODEL).

References

[1] Alur, R., Courcoubetis, C., Dill, D.L., Halbwachs, N., Wong-Toi, H.: An implementation of three algorithms for timing verification based on automata emptiness. In: RTSS. pp. 157–166. IEEE Computer Society (1992)

[2] Alur, R., Dill, D.L.: A theory of timed automata. Theor. Comput. Sci. **126**(2), 183–235 (1994)

[3] Alur, R., La Torre, S., Pappas, G.J.: Optimal paths in weighted timed automata. In: HSCC. Lecture Notes in Computer Science, vol. 2034, pp. 49–62. Springer (2001)

[4] Behrmann, G., Cougnard, A., David, A., Fleury, E., Larsen, K.G., Lime, D.: Uppaal-tiga: Time for playing games! In: CAV. Lecture Notes in Computer Science, vol. 4590, pp. 121–125. Springer (2007)

[5] Behrmann, G., Fehnker, A., Hune, T., Larsen, K.G., Pettersson, P., Romijn, J., Vaandrager, F.W.: Minimum-cost reachability for priced timed automata. In: HSCC. Lecture Notes in Computer Science, vol. 2034, pp. 147–161. Springer (2001)

[6] Behrmann, G., Larsen, K.G., Rasmussen, J.I.: Priced timed automata: Algorithms and applications. In: FMCO. Lecture Notes in Computer Science, vol. 3657, pp. 162–182. Springer (2004)

[7] Bouyer, P., Brinksma, E., Larsen, K.G.: Staying alive as cheaply as possible. In: HSCC. Lecture Notes in Computer Science, vol. 2993, pp. 203–218. Springer (2004)

[8] Bouyer, P., Brinksma, E., Larsen, K.G.: Optimal infinite scheduling for multi-priced timed automata. Formal Methods Syst. Des. **32**(1), 3–23 (2008)

[9] Bouyer, P., Cassez, F., Fleury, E., Larsen, K.G.: Optimal strategies in priced timed game automata. In: FSTTCS. Lecture Notes in Computer Science, vol. 3328, pp. 148–160. Springer (2004)

[10] Bozga, M., Daws, C., Maler, O., Olivero, A., Tripakis, S., Yovine, S.: Kronos: A model-checking tool for real-time systems. In: CAV. Lecture Notes in Computer Science, vol. 1427, pp. 546–550. Springer (1998)

[11] Bozkurt, A.K., Wang, Y., Zavlanos, M.M., Pajic, M.: Control synthesis from linear temporal logic specifications using model-free reinforcement learning. In: 2020 IEEE International Conference on Robotics and Automation, ICRA 2020, Paris, France, May 31 - August 31, 2020. pp. 10349–10355. IEEE (2020). https://doi.org/10.1109/ICRA40945.2020.9196796, `https://doi.org/10.1109/ICRA40945.2020.9196796`

[12] Camacho, A., Icarte, R.T., Klassen, T.Q., Valenzano, R.A., McIlraith, S.A.: LTL and beyond: Formal languages for reward function specification in reinforcement learning. In: Proceedings of the Twenty-Eighth International Joint Conference on Artificial Intelligence, IJCAI 2019, Macao, China, August 10-16, 2019. pp. 6065–6073. ijcai.org (2019). https://doi.org/10.24963/IJCAI.2019/840, `https://doi.org/10.24963/ijcai.2019/840`

[13] Cohen, M.H., Belta, C.: Model-based reinforcement learning for approximate optimal control with temporal logic specifications. In: HSCC. pp. 12:1–12:11. ACM (2021)

[14] Corazza, J., Gavran, I., Neider, D.: Reinforcement learning with stochastic reward machines. In: AAAI. pp. 6429–6436. AAAI Press (2022)

[15] David, A., Jensen, P.G., Larsen, K.G., Mikucionis, M., Taankvist, J.H.: Uppaal stratego. In: TACAS. Lecture Notes in Computer Science, vol. 9035, pp. 206–211. Springer (2015)

[16] Dole, K., Gupta, A., Komp, J., Krishna, S., Trivedi, A.: Event-triggered and time-triggered duration calculus for model-free reinforcement learning. In: RTSS. pp. 240–252. IEEE (2021)

[17] Dole, K., Gupta, A., Komp, J., Krishna, S., Trivedi, A.: Correct-by-construction reinforcement learning of cardiac pacemakers from duration calculus requirements. In: AAAI. pp. 14792–14800. AAAI Press (2023)

[18] Falah, A., Guha, S., Trivedi, A.: Reinforcement learning for omega-regular specifications on continuous-time MDP. In: ICAPS. pp. 578–586. AAAI Press (2023)

[19] Falah, A., Guha, S., Trivedi, A.: Continuous-time reward machines. In: IJCAI. pp. 5056–5064. ijcai.org (2025)

[20] Fujimoto, S., van Hoof, H., Meger, D.: Addressing function approximation error in actor-critic methods. In: ICML. Proceedings of Machine Learning Research, vol. 80, pp. 1582–1591. PMLR (2018)

[21] Hahn, E.M., Perez, M., Schewe, S., Somenzi, F., Trivedi, A., Wojtczak, D.: Omega-regular reward machines. In: ECAI. Frontiers in Artificial Intelligence and Applications, vol. 372, pp. 972–979. IOS Press (2023)

[22] Hasanbeig, M., Kantaros, Y., Abate, A., Kroening, D., Pappas, G.J., Lee, I.: Reinforcement learning for temporal logic control synthesis with probabilistic satisfaction guarantees. In: 58th IEEE Conference on Decision and Control, CDC 2019, Nice, France, December 11-13, 2019. pp. 5338–5343. IEEE (2019). https://doi.org/10.1109/CDC40024.2019.9028919, `https://doi.org/10.1109/CDC40024.2019.9028919`

[23] Henzinger, T.A., Manna, Z., Pnueli, A.: What good are digital clocks? In: ICALP. Lecture Notes in Computer Science, vol. 623, pp. 545–558. Springer (1992)

[24] Icarte, R.T.: Reward Machines. Ph.D. thesis, University of Toronto, Canada (2022)

[25] Icarte, R.T., Klassen, T.: Reward machines. `https://github.com/RodrigoToroIcarte/reward_machines` (2018), gitHub repository

[26] Icarte, R.T., Klassen, T.Q., Valenzano, R.A., McIlraith, S.A.: Using reward machines for high-level task specification and decomposition in reinforcement learning. In: ICML. Proceedings of Machine Learning Research, vol. 80, pp. 2112–2121. PMLR (2018)

[27] Icarte, R.T., Klassen, T.Q., Valenzano, R.A., McIlraith, S.A.: Reward machines: Exploiting reward function structure in reinforcement learning. J. Artif. Intell. Res. **73**, 173–208 (2022). https://doi.org/10.1613/JAIR.1.12440, `https://doi.org/10.1613/jair.1.12440`

[28] Icarte, R.T., Waldie, E., Klassen, T.Q., Valenzano, R.A., Castro, M.P., McIlraith, S.A.: Learning reward machines for partially observable reinforcement learning. In: NeurIPS. pp. 15497–15508 (2019)

[29] Jothimurugan, K., Bansal, S., Bastani, O., Alur, R.: Compositional reinforcement learning from logical specifications. In: NeurIPS. pp. 10026–10039 (2021)

[30] Kane, A., Chowdhury, O., Datta, A., Koopman, P.: A case study on runtime monitoring of an autonomous research vehicle (ARV) system. In: RV. Lecture Notes in Computer Science, vol. 9333, pp. 102–117. Springer (2015)

[31] Larsen, K.G., Pettersson, P., Yi, W.: UPPAAL in a nutshell. Int. J. Softw. Tools Technol. Transf. **1**(1-2), 134–152 (1997)

[32] Neary, C., Xu, Z., Wu, B., Topcu, U.: Reward machines for cooperative multi-agent reinforcement learning. In: AAMAS. pp. 934–942. ACM (2021)

[33] Puterman, M.L.: Markov Decision Processes: Discrete Stochastic Dynamic Programming. Wiley Series in Probability and Statistics, Wiley (1994)

[34] Shao, D., Kwiatkowska, M.: Sample efficient model-free reinforcement learning from LTL specifications with optimality guarantees. In: IJCAI. pp. 4180–4189. ijcai.org (2023)

[35] Sutton, R.S., Barto, A.G.: Reinforcement learning - an introduction, 2nd Edition. MIT Press (2018)

[36] Tollund, R.G., Johansen, N.S., Nielsen, K.Ø., Torralba, Á., Larsen, K.G.: Optimal infinite temporal planning: Cyclic plans for priced timed automata. In: ICAPS. pp. 588–596. AAAI Press (2024)

[37] Towers, M., Kwiatkowski, A., Terry, J., Balis, J.U., De Cola, G., Deleu, T., Goulão, M., Kallinteris, A., Krimmel, M., KG, A., Perez-Vicente, R., Pierré, A., Schulhoff, S., Tai, J.J., Tan, H., Younis, O.G.: Gymnasium: A standard interface for reinforcement learning environments. arXiv preprint arXiv:2407.17032 (2024)

[38] Watkins, C.J.C.H., Dayan, P.: Technical note q-learning. Mach. Learn. **8**, 279–292 (1992)

[39] Xu, Z., Topcu, U.: Transfer of temporal logic formulas in reinforcement learning. In: IJCAI. pp. 4010–4018. ijcai.org (2019)